Chinese Chemical Letters 33 (2022) 239–242

Contents lists available at ScienceDirect

Chinese Chemical Letters

journal homepage: www.elsevier.com/locate/cclet

Accelerating the thermal fading rate of photochromic naphthopyrans by pillar[5]arene-based conjugated macrocycle polymer

Shuangyan Liu[a,1], Taishan Yan[b,1], Qiuxia Wu[b], Zheng Xu[a], Jie Han[a,b,*]

[a] Key Laboratory of Advanced Energy Materials Chemistry (Ministry of Energy), College of Chemistry, Nankai University, Tianjin 300071, China
[b] State Key Laboratory of Elemento-Organic Chemistry, College of Chemistry, Nankai University, Tianjin 300071, China

ARTICLE INFO

Article history:
Received 23 March 2021
Revised 5 July 2021
Accepted 8 July 2021
Available online 14 July 2021

Keywords:
Pillar[5]arene
Conjugated macrocycle polymer
Naphothopyran
Photochromism
Thermal fading rate
Matrix effect

ABSTRACT

A new micro-spherical conjugated macrocycle polymer (P[5]-TFB-CMP) was prepared by the condensation reaction between dihydrazide functionalized pillar[5]arene and 1,3,5-triformylbenzene under ambient conditions. P[5]-TFB-CMP exhibits large surface area with excellent thermal stability and has been used as additive to prepare composite PMMA film of photochromic naphthopyrans. The results showed that the addition of P[5]-TFB-CMP could dramatically accelerate the thermal fading rate of the photochromic composite film by up to 12 times. This is a new strategy to overcome the drawback of the matrix effect.

Among many kinds of photochromic compounds [1-4], naphthopyran derivatives have drawn continuous interest due to the various applications in many fields such as ophthalmic lenses [5,6], smart windows [7] and textiles [8,9]. Generally, several parameters including the color, optical density, fatigue resistance and thermal fading rate are key factors to evaluate the performance of photochromic naphtopyrans. As the thermal fading rates of most photochromic naphthopyrans are not fast enough to face the practical performance requirements, it is an important task to accelerate the fading rate of such kind of photo-functional materials [10,11]. Particularly, the practical application in ophthalmic lenses requires that the photochromic compounds should be incorporated into the polymer host/substrate. However, when photochromic molecules are incorporated into a polymer matrix, the thermal fading rate is much slower than that can be achieved in solution, because the limited free volume of polymer host might restrict the movements of photochromic molecules and make it difficult for the photochemical reactions. This phenomenon is also known as the matrix effect [12]. Several methods have been reported to overcome the drawback of matrix effect [13-15]. However, this issue has not been solved, and efficient methods to improve the thermal fading rate of photochromic materials in polymer matrix are still limited at present.

Porous organic polymers such as covalent organic frameworks [16], porous aromatic frameworks [17] and conjugated microporous polymers [18,19] have drawn great interest in recent years, as they have been widely used in many fields including gas adsorption and separation, organic photoelectric materials, cathode materials and separation membrane materials. Among various porous organic polymers, the pillararene-based conjugated macrocycle polymers [20-23] (PCMPs) are special in that the introduction of pillararene [24-26] to CMPs can form two types of porosity, *i.e.*, one from the cross-linked pores of the CMPs and the other from the intrinsic cavity of the pillararene, which may combine the advantages of macrocyclic hosts and the virtues of solid porous polymers. The unique features of the hierarchically porous materials may lead into some novel functions. Although much progress has been achieved in pillararene-based supramolecular polymers [27-31], only several examples of PCMPs have been reported up to now. In 2016, Müllen *et al.* first reported a fishing rod-like conjugated polymer bearing pillar[5]arenes with high fluorescent intensity both in solution and in solid state [32], Nearly at the same time, by the similar synthetic strategy Coskun and co-workers prepared another pillar[5]arene based conjugated microporous polymer for propane/methane separation [33]. In 2018, Yang's group reported two conjugated macrocycle polymers (P[5]-TPE-CMP and P[5]-TET-CMP) based on pillar[5]arene and found that P[5]-TPE-CMP could be used as two-photon fluorescence sensors for metal

* Corresponding author at: Key Laboratory of Advanced Energy Materials Chemistry (Ministry of Energy), College of Chemistry, Nankai University, Tianjin 300071, China.
E-mail address: hanjie@nankai.edu.cn (J. Han).
[1] These authors have contributed equally to this work.

https://doi.org/10.1016/j.cclet.2021.07.023
1001-8417/

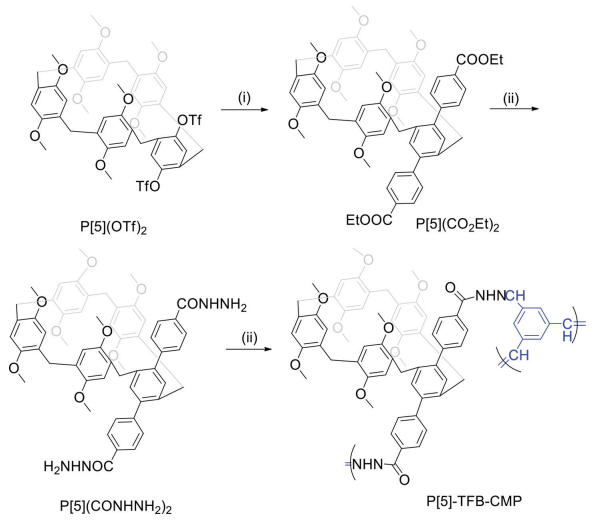

Scheme 1. Synthetic route to P[5]-TFB-CMP: (i) (4-(ethoxycarbonyl)phenyl)boronic acid, $Pd(PPh_3)_4$, Na_2CO_3, THF/H_2O, 80 °C, 72 h, 74%; hydrazine hydrate, EtOH, reflux, 48 h, 91%; (iii) 1,3,5-triformylbenzene,1,4-dioxane, mesitylene, HOAc (6 mol/L), r.t., 72 h, 78%.

ions and organic molecules [34], while Wen's group discovered that P[5]-TET-CMP showed unique photocatalytic selectivity for oxidization of sulfides [35]. Very recently, Tang, Cao and co-workers prepared a conjugated polymeric supramolecular network through the self-assembly of a pillar[5]arene-based CMP and conjugated ditopic guests, and found that CPSNs could be acted as artificial light-harvesting systems with unprecedented antenna effect [36]. The development of new functional PCMPs might draw wide interest from many fields such as supramolecular chemistry and material sciences.

In this communication, we would like to report a new pillar[5]arene-based conjugated macrocycle polymer (P[5]-TFB-CMP), which is constructed from dihydrazide-functionalized pillar[5]arene P[5]$(CONHNH_2)_2$ and 1,3,5-triformylbene (Scheme 1). The time dependent ^1H NMR of P[5]$(CONHNH_2)_2$ and 1,3,5-triformylbenzene is shown in Fig. S11 (Supporting information), indicating that P[5]$(CONHNH_2)_2$ and 1,3,5-triformylbene could completely convert to P[5]-TFB-CMP in about 72 h. The product P[5]-TFB-CMP was further used to prepare a composite polymethyl methacrylate (PMMA) film with photochromic naphthopyrans. Notably, it is found that the thermal fading rate could be accelerated dramatically by twelve times. This is a new strategy to overcome the drawback of polymer matrix.

The intermediates P[5]$(CO_2Et)_2$ and P[5]$(CONHNH_2)_2$ were synthesized and fully characterized by means of ^1H NMR, ^{13}C NMR and high resolution mass spectroscopy (details see Supporting information). The pillar[5]arene-based conjugated macrocycle polymer P[5]-TFB-CMP was prepared according to the following procedures. Dihydrazide functionalized pillar[5]arene P[5]$(CONHNH_2)_2$, 1,3,5-triformylbenzene, and aqueous HOAc were added to a vial and suspended in a mixture of 1,4-dioxane and mesitylene. The mixture was kept still for 72 h, then the as-formed white solid was isolated by filtration, washed with acetone and tetrahydrofuran and further purification by Soxhlet extraction for 24 h to afford P[5]-TFB-CMP. This is a typical procedure reported by Wang for preparing covalent organic frameworks [37]. Initially, we anticipated to get highly ordered covalent organic frameworks, however, our product is non-crystalline microporous material as discussed in the following. This might be explained by the presence of the nonplanar and steric pillar[5]arene, which was proposed to hinder the formation of crystalline structure [38].

P[5]-TFB-CMP sample was acquired as a white powder, and was found to be absolutely undissolving in common organic solvents, such as *N,N*-dimethylformamide, dimethylsulfoxide, dichloromethane, *N*-methyl-2-pyrrolidone, acetone, ethyl acetate, tetrahydrofuran, and ethanol, strongly indicating the formation of a cross-linked structure. The molecular level connectivity of P[5]-TFB-CMP was assessed by Fourier transform infrared (FT-IR) spectroscopy and solid-state cross-polarization magic angle spinning (CP/MAS) ^{13}C NMR spectroscopy. The FT-IR spectra (Fig. 1) showed two characteristic vibrational bands at 1609 and 1229 cm^{-1} associated with the formation of the –C=N– bonds [39]. It is notable that the stretching hands arising from amine (3314 cm^{-1}) and aldehyde (1686 cm^{-1}) largely decreased or even disappeared in comparison to those of P[5]$(CONHNH_2)_2$ and 1,3,5-triformylbenzene, also verifying the effective condensation reaction between the two reactive precursors. The solid-state CP/MAS ^{13}C NMR spectrum (Fig. S12 in Supporting information) of P[5]-TFB-CMP showed an intense signal at 151 ppm, corresponding to the carbons in C=N bonds [40], while the aldehyde carbon signal [41] was dramatically decreased, further indicating the construction of conjugated macrocycle polymers.

The scanning electron microscopy (SEM) image (Fig. 1b) and the dynamic light scattering (DLS) experiment (Fig. S18 in Supporting information) of P[5]-TFB-CMP revealed its morphology as nearly uniform spheres with about 1 micrometer scale. This might be explained as cross edge-to-edge interaction of precursors leading to a curved architecture, which on cross-linkage formed a spherical morphology [42,43]. The high-angle annular dark-field scanning transmission electron microscopy (HAADF-STEM) studies further confirmed the spherical morphology (Fig. 1c) of P[5]-TFB-CMP, which remains unblemished under the electron beam. The selected area electron diffraction (SAED) image and corresponding elemental mappings indicate the homogeneous distribution of C, N and O within the material, and the dot patterns in the SAED image of an individual ferrite octahedron confirmed its good crystallinity (Figs. S19a-d in Supporting information). The broad peaks in powder X-ray diffraction pattern (Fig. S20 in Supporting information) of P[5]-TFB-CMP suggested its spherical structure, which is consistent with the SEM and TEM results.

The porosity of P[5]-TFB-CMP was investigated by nitrogen adsorption and desorption analysis at 77 K (Fig. 2a), which exhibits a characteristic type IV shape, indicating the presence of microporosity. A linear increase in nitrogen sorption isotherm with relative pressure at P/P_0 = 0.01–0.29 and the hysteresis curve suggested that the mechanism of adsorption/desorption is reversible in nature (Fig. S21 in Supporting information). The total pore volume was determined to be 0.38 cm^3/g on the basis of a single point measurement at P/P_0 = 0.99, and the adsorption average pore diameter (4V/A by BET) was 6.3 nm (Fig. 2b). The Brunauer-Emmett-Teller (BET) surface area of P[5]-TFB-CMP was calculated to be 240.8 m^2/g, which was much higher than that (6.99 m^2/g) of the reported conjugated macrocycle polymer constructed from pillar[5]arene and tetrakis(4-ethynylphenyl) ethylene [34]. Thermogravimetric analysis (TGA) revealed thermal stability of P[5]-TFB-CMP is up to 360 °C in nitrogen atmosphere, then the TGA curve decreased gradually, indicating the sample decomposed gradually with the increase of the temperature (Fig. 2c). The larger surface area, porous nature with spherical morphology and excellent thermal stability may provide potential volume for adsorption of some special photochromic naphthopyans and accelerate the thermal fading rate.

In order to investigate the effect of P[5]-TFB-CMP on the thermal fading rate, a widely studied naphthopyran compound, 2,2-bis(4-methoxyphenyl)-2*H*-benzo[h]chromene (**NP1**), was prepared according to the method in literature [44]. It is well known that the alkylnitrile compounds had very strong binding affinities with

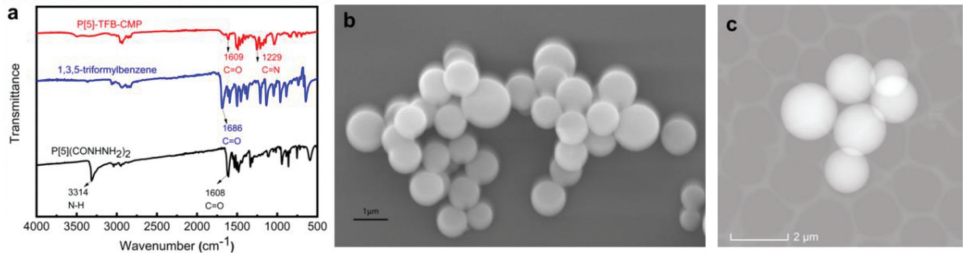

Fig. 1. (a) FT-IR spectra of 1,3,5-triformylbenzene, P[5]-TFB-CMP and P[5](CONHNH$_2$)$_2$; (b) SEM image of P[5]-TFB-CMP; (c) HAADF-STEM image of P[5]-TFB-CMP.

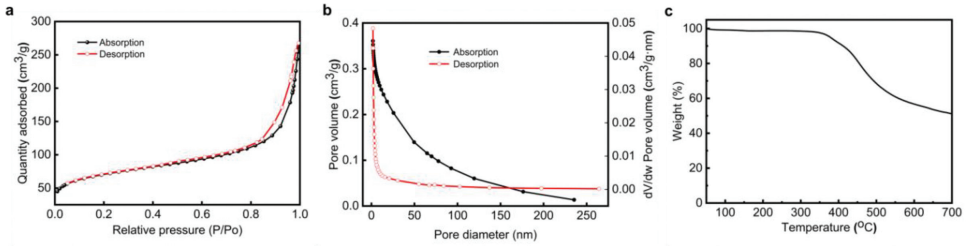

Fig. 2. (a) N_2 adsorption-desorption isotherms of P[5]-TFB-CMP; (b) pore size distribution of P[5]-TFB-CMP; (c) TGA curve of P[5]-TFB-CMP under the nitrogen atmosphere.

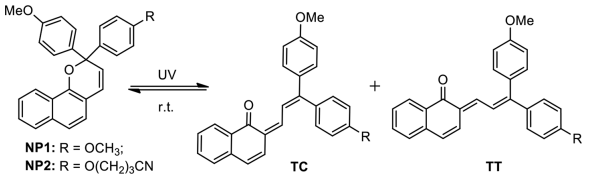

Scheme 2. the molecular structures of **NP1** and **NP2** as well as the photochromic mechanism.

the pillararene based on the cooperative multiple hydrogen bond and dipole-dipole interactions to form various supramolecular systems [45]. For comparison, a new photochromic naphthopyran derivative (**NP2**) with a cyanobutoxy group was synthesized with the detailed procedures showing in the supporting information. The molecular structures of **NP1** and **NP2** as well as the photochromic mechanism are shown in Scheme 2. Upon irradiation with UV light, the colorless closed form (CF) of the naphthopyrans generates the colored *transoid-cis* (TC) and the *transoid-trans* (TT) *via* the cleavage of the pyran C–O bond; when the light source is turned off, both opened colored species thermally revert to the initially closed form and restore the colorless state. Generally, the TT form tends to take longer time (from minutes to hours) to thermally transform into the close form than the TC form does (from seconds to minutes).

The composite PMMA films doped with **NP1, NP2** and P[5]-TFB-CMP, namely, **NP1**⊂PMMA, **NP1**⊂P[5]-TFB-CMP⊂ PMMA, **NP2**⊂PMMA, and **NP2**⊂P[5]-TFB-CMP⊂PMMA were prepared to explore the effect of the P[5]-TFB-CMP on the thermal fading rate of **NP1** and **NP2**. The detailed procedures for the preparation of composite films are shown in the supporting information. With the samples at hands, we first examined the absorption spectra of **NP2**⊂PMMA⊂P[5]-TFB-CMP over 200–700 nm as shown in Fig. S22 (Supporting informaiton). Upon irradiation with 365 nm UV light, a new absorption with the maximum absorption wavelength (λ_{max}) at 500 nm appeared, which is also the strongest absorption. The thermal fading kinetics of the photochromic composite films were measured by monitoring the absorption of the sample versus time at the maximum of the absorption band (Figs. 3a and b, and Figs. S24a and b in Supporting information). The kinetic constants are summarized in Table 1. The kinetic constants k_1 and k_2 are calculated from the bleaching curves using a bi-exponential decay equation: $A(t) = A_1 e^{-k_1 t} + A_2 e^{-k_2 t} + A_{th}$ [46-47], where $A(t)$ is

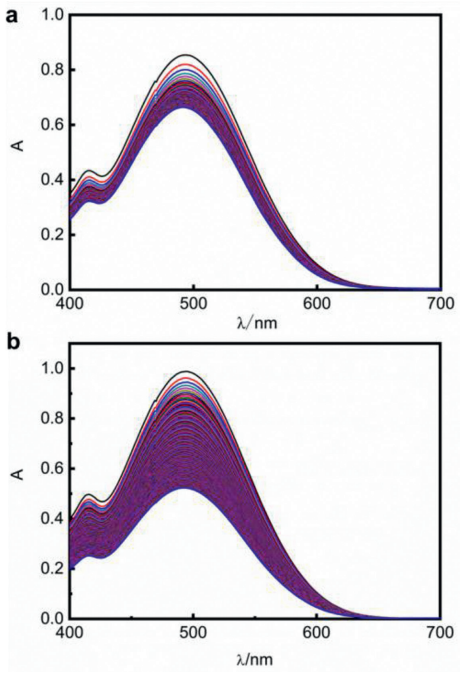

Fig. 3. Absorption spectral changes (the time internal is 20 s) of the composite film: (a) **NP1**⊂PMMA and (b) **NP1**⊂P[5]-TFB-CMP⊂PMMA.

the optical density at λ_{max} of the opened forms, A_1 and A_2 are the contributions to the initial optical density, and A_{th} is the residual coloration at the termination of the testing time. The $t_{1/2}$ value, which is the time taken for the sample to fade to half of the initial absorbance value, is used to compare overall kinetics. Our study of the decay kinetics of colored forms indicated the excellent agreement between the biexponential model and the experimental data (Figs. S23, S24c and d in Supporting information). As seen in Table 1, the wavelengths of the absorption maximum (λ_{max}) of **NP1**⊂PMMA and **NP1**⊂P[5]-TFB-CMP⊂PMMA are almost the same, meaning the addition of P[5]-TFB-CMP nearly has no effect on the color of the photochromic films. In sharp contrast, the fading rate of **NP1**⊂P[5]-TFB-CMP⊂PMMA is increased dramatically by more than twelve times of that of **NP1**⊂PMMA (29.3 min *vs.* 360.4 min). The possible reason is that the cross-linked pores of P[5]-TFB-CMP

Table 1
Kinetic data of the photochromic composite films.

Sample	λ_{max} (nm)	$t_{1/2}$ (min)	k_1 (min^{-1})	k_2 (min^{-1})	A_1	A_2	A_{th}
NP1⊂PMMA	494	360.4	0.008	0.00018	0.216	0.103	0.679
NP1⊂P[5]-TFB-CMP⊂PMMA	495	29.3	0.005	0.00033	0.310	0.373	0.334
NP2⊂PMMA	493	865.3	0.006	0.00015	0.124	0.088	0.621
NP2⊂P[5]-TFB-CMP⊂PMMA	494	98.0	0.003	0.00015	0.144	0.545	0.273

might provide large space enough for the open forms of naphthopyrans to revert to the initially close form, and consequently accelerate the color fading rate. However, the in-depth reason is not clear at present. As the conjugated structures of **NP1** and **NP2** are same to each other, it is easy to understand that both **NP2**⊂PMMA and **NP2**⊂P[5]-TFB-CMP⊂PMMA exhibit similar wavelengths of the absorption maximum to those of **NP1**⊂PMMA and **NP1**⊂P[5]-TFB-CMP⊂PMMA. Compared to **NP1**⊂PMMA, **NP2**⊂PMMA exhibited much slow fading rate. This is probably because that the large molecular structure of **NP2** due to the cyanobutoxy group is not facilitated to the photochemical reactions in the limited space of the composite film. Same as expected, the addition of P[5]-TFB-CMP also accelerated the fading rate of the composite film of **NP2**, but the effect is a little weaker than that of **NP1**. The host-guest interactions between the cyanobutoxy group of **NP2** and the pillar[5]arene cavity of P[5]-TFB-CMP might hinder the back reactions from the TC and TT forms of **NP2**, which might be explained reasonably the fact that the color fading rate of **NP2**⊂P[5]-TFB-CMPÌPMMA is slower than that of **NP1**⊂P[5]-TFB-CMP⊂PMMA.

In conclusion, we have synthesized and characterized a hydrazone-linked conjugated macrocycle polymer, P[5]-TFB-CMP, by the condensation reaction between dihydrazide functionalized pillar[5]arene and 1,3,5-triformylbenzene under ambient conditions. P[5]-TFB-CMP exhibited uniform micro-spherical morphology with large surface area and excellent thermal stability, which has been successfully used as additive to the PMMA films of photochromic naphthopyrans. The addition of P[5]-TFB-CMP could dramatically accelerate the fading rate of the photochromic composite film up to 12 times. This work provides an efficient method to overcome the drawback of the matrix effect.

Declaration of competing interest

The authors declare that they have no known competing financial interests or personal relationships that could have appeared to influence the work reported in this paper.

Acknowledgments

The work was financially supported by Natural Science Foundation of Tianjin (No. 18JCYBJC20700) and the 111 Project (No. B12015).

Supplementary materials

Supplementary material associated with this article can be found, in the online version, at doi:10.1016/j.cclet.2021.07.023.

References

[1] H. Chen, W. Chen, Y. Lin, et al., Chin. Chem. Lett. 32 (2021) 2359–2368.
[2] C. Xiao, W.Y. Zhao, D.Y. Zhou, et al., Chin. Chem. Lett. 31 (2020) 361–364.
[3] A. Mukhopadhyay, J.N. Moorthy, J. Photochem. Photobio. C 29 (2016) 73–106.
[4] C. Xiao, W.Y. Zhao, D.Y. Zhou, et al., Chin. Chem. Lett. 26 (2015) 817–824.
[5] C.M. Sousa, P.J. Coelho, Eur. J. Org. Chem. 85 (2020) 985–992.
[6] N. Malic, J.A. Campbell, A.S. Ali, et al., Macromolecules 43 (2010) 8488–8501.
[7] K. Klaue, Y. Garmshausen, S. Hecht, Angew. Chem. Int. Ed. 57 (2018) 1414–1417.
[8] T.V. Pinto, P. Costa, C.M. Sousa, et al., ACS Appl. Mater. Interfaces 8 (2016) 28935–28945.
[9] M. Aldib, R.M. Christie, Color. Technol. 127 (2011) 282–287.
[10] H. Kuroiwa, Y. Inagaki, K. Mutoh, J. Abe, Adv. Mater. 30 (2018) 1805661.
[11] C.M. Sousa, J. Berthet, S. Delbaere, A. Polónia, P.J. Coelho, J. Org. Chem. 82 (2017) 12028–12037.
[12] V. Krongauz, Environment effects on organic photochromic systems, in H. Dürr, H. Bouas-Laurent (Eds.), Photochromism: Molecules and System, 1st Ed., Elsevier Publishing House, Amsterdam, 1990, pp 793-820.
[13] F. Ercole, N. Malic, S. Harrisson, T.P. Davis, R.A. Evans, Macromolecules 43 (2010) 249–261.
[14] P.J. Coelho, C.J.R. Silva, C. Sousa, S.D.F.C. Moreira, J. Mater. Chem. C 1 (2013) 5387–5394.
[15] K. Mutoh, Y. Kobayashi, J. Abe, Dyes Pigm. 137 (2017) 307–311.
[16] A.P. Cote, A.I. Benin, N.W. Ockwig, et al., Science 310 (2005) 1166–1170.
[17] T. Ben, H. Ren, S. Ma, et al., Angew. Chem. Int. Ed. 48 (2009) 9457–9460.
[18] J. Han, X. Fan, Z.-Z. Zhuang, et al., RSC Adv. 5 (2015) 15350–15353.
[19] Y. Xu, S. Jin, H. Xu, A. Nagai, D. Jiang, Chem. Soc. Rev. 42 (2013) 8012–8031.
[20] X. Yan, Y. Huang, M. Cen, et al., Nanoscale Adv. 3 (2021) 1906–1909.
[21] R. Zhang, X. Yan, H. Guo, et al., Chem. Commun. 56 (2020) 948–951.
[22] Y. Deng, X. Li, C. Han, S. Dong, Chin. Chem. Lett. 31 (2020) 3221–3224.
[23] X. Zhang, X. Wang, B. Wang, Z.J. Ding, C. Li, Chin. Chem. Lett. 31 (2020) 3230–3232.
[24] T. Xiao, L. Xu, W. Zhong, et al., Isr. J. Chem. 58 (2018) 1183–1193.
[25] T. Xiao, L. Qi, W. Zhong, et al., Mater. Chem. Front. 3 (2019) 1973–1993.
[26] T. Xiao, L. Zhou, L. Xu, et al., Chin. Chem. Lett. 30 (2019) 271–276.
[27] S. Liu, Q. Wu, T. Zhang, H. Zhang, J. Han, Org. Biomol. Chem. 19 (2021) 1287–1291.
[28] H. Li, W. Chen, F. Xu, et al., Macromol. Rapid Commun. 39 (2018) 1800053.
[29] X.Y. Yang, W.Q. Cai, S. Dong, et al., ACS Macro Lett. 6 (2017) 647–651.
[30] J.F. Chen, Q. Lin, Y.M. Zhang, H. Yao, T.B. Wei, Chem. Commun. 53 (2017) 13296–13311.
[31] S.L. Wang, Y.L. Wang, Z.X. Chen, et al., Chem. Commun. 51 (2015) 3434–3437.
[32] Y. Ma, L. Chen, C. Li, K. Müllen, Chem. Commun. 52 (2016) 6662–6664.
[33] S.N. Talapaneni, D. Kim, G. Barin, et al., Chem. Mater. 28 (2016) 4460–4466.
[34] X. Li, Z. Li, Y.W. Yang, Adv. Mater. 30 (2018) 1800177.
[35] H. Qiang, T. Chen, Z. Wang, et al., Chin. Chem. Lett. 31 (2020) 3225–3229.
[36] L. Xu, Z. Wang, R. Wang, et al., Angew. Chem. Int. Ed. 59 (2020) 9908–9913.
[37] S.Y. Ding, X.H. Cui, J. Feng, G. Lu, W. Wang, Chem. Commum. 53 (2017) 11950–11959.
[38] C.M. Thompson, G. Occhialini, G.T. McCandless, et al., J. Am. Chem. Soc. 139 (2017) 10506–10513.
[39] Y. Yan, X. Li, G. Chen, et al., Chem. Chem. Lett. 32 (2021) 107–122.
[40] Z.J. Li, S.Y. Ding, H.D. Xie, W. Cao, W. Wang, Chem. Commun. 52 (2016) 7217–7220.
[41] F.J. Uribe-Romo, C.J. Doonan, H. Furukawa, K. Oisaki, O.M. Yaghi, J. Am. Chem. Soc. 133 (2011) 11478–11481.
[42] K.Prakash Subodh, D.T. Masram, J. Mater. Chem. C 8 (2020) 9201–9204.
[43] S. Kandambeth, V. Venkatesh, D.B. Shinde, et al., Nat. Commun. 6 (2015) 6786.
[44] C.D. Gabbutt, B.M. Heron, A.C. Instone, et al., Eur. J. Org. Chem. (2003) 1220–1230.
[45] N. Song, D.X. Chen, M.C. Xia, et al., Chem. Commun. 51 (2015) 5526–5529.
[46] J. Biteau, F. Chaput, J.P. Boilot, J. Phys. Chem. 100 (1996) 9024–9031.
[47] Y. Zhang, G. Wang, J. Zhang, Tetrahedron 70 (2014) 5966–5973.